Detection and Assessment of Partial Shading Scenarios on Photovoltaic Strings

Jieming Ma, *Member, IEEE,* Xinyu Pan, Ka Lok Man, Xingshuo Li, Huiqing Wen, *Member, IEEE,* and Tiew On Ting, *Member, IEEE*

***Abstract*—There has been growing interest in using photovoltaic (PV) energy harvesting technology to reduce reliance on mineral-based energy. Partial shading scenarios (PSS) significantly affect the electrical characteristics of a PV generator. However, few studies have devoted to the detection and assessment of the PSS. In this paper, shading rate and shading strength are used to characterize the PSS. A shading pattern detection algorithm is proposed to estimate the number of shaded modules in a PV string and distinguish the PSS from uniform irradiation scenarios. A multiple-output support vector regression (M-SVR) is applied to estimate the shading strength. In addition, the maximum power point voltage of the applied PV generation system can be predicted from measured data. Simulation and experimental validation show the feasibility of the proposed method in the face of various environmental conditions. It could be used as a preliminary step toward automatic supervision and monitoring PV generation system.**

***Keywords*—Photovoltaic cells, partial shading conditions, measurement, partial shading detection, support vector regression.**

NOMENCLATURE

V	Terminal voltage of a photovoltaic (PV) module (V).
I	Terminal current of a PV module (A).
V_S	Terminal voltage of a PV string (V).
I_S	Terminal current of a PV string (A).
I-V	Relationship between current and voltage.
P-V	Relationship between power and voltage.
$V - V_S$	Relationship between module voltage and string voltage.
I_{ph}	Light-generated current of a PV module (A).
I_o	Reverse saturation current of the diode (A).
a	Ideality factor of a PV module.
r_s	Series resistance of a PV module (Ω).
r_p	Parallel resistance of a PV module (Ω).
V_t	Thermal voltage of a PV module (V).
B	Boltzmann constant (J/K).
e	Electron charge (C).
n_s	The number of PV cells in a PV module.
R_s	Terminal voltage of a PV string (V).
R_p	Terminal current of a PV string (A).
N_S	The number of PV modules in a PV string.
T	Temperature (^oC).
N_{sh}	The number of shaded modules in a PV string.
M	Photovoltaic module number.
G_{sh}	Irradiance received by shaded modules (W/m^2).
G_{is}	Irradiance received by insolated modules (W/m^2).
ρ	Shading strength.
χ	Shading rate.
V_{mp}	Voltage at the maximum power point of a PV module.
$V_{S,mp}$	Voltage at the maximum power point of a PV string.
V_{oc}	Open circuit voltage (V).
ΔV_{oc}	Difference of the open circuit voltage between shaded and insolated modules (V).
V_{det}	Normalization of V_{sort} (V).
V_{sort}	Sorted voltage vector (V).
A	The vector to be sorted.
p, q, r	Variables used in the proposed shading pattern detection algorithm.
τ	The threshold used to differentiate between the uniform illumination scenarios and partial shading scenarios.
x_k	The k^{th} input data of a support vector regression (SVR) model.
y_k	The regression value associated with x_k.
ξ_k, ξ_k^*	Slack variables used in a SVR model.
C	Positive trade-off penalty for slack variables.
w	Weight vector of a SVR model.
b	Bias used in a SVR model.
α_k, α_k^*	Lagrange multipliers associated with x_k.
ε	Tube tolerance width.
K	Kernel matrix.
ϕ	Kernelized mapping function.
σ	Tuning parameter defining the kernel width.
C_{max}, C_{min}	Maximum and minimum values of C.

J. Ma is with the Department of Computer Science and Software Engineering, Xi'an Jiaotong-Liverpool University, Suzhou, 215123 P.R. China, and School of Electronic and Information Engineering, Suzhou University of Science and Technology, Suzhou 215009, P.R. China. e-mail: jieming84@gmail.com

Xinyu Pan is with the School of Electronic and Information Engineering, Suzhou University of Science and Technology, Suzhou 215009, P.R. China. e-mail:panxy@mail.usts.edu.cn.

K. L. Man is with the Department of Computer Science and Software Engineering, Xi'an Jiaotong-Liverpool University, Suzhou, 215123 P.R. China, and Faculty of Engineering, Computing and Science, Swinburne University of Technology, Q5A 93300 Kuching, Sarawak, Malaysia. e-mail: ka.man@xjtlu.edu.cn.

X. Li, H. Wen, and T.O. Ting are with the Department of Electrical and Electronic Engineering, Xi'an Jiaotong-Liverpool University, Suzhou, 215123 P.R. China. e-mail: xingshuo.li@xjtlu.edu.cn; huiqing.wen@xjtlu.edu.cn; toting@xjtlu.edu.cn.

Manuscript received Oct 1, 2017; revised **, 2017.

$\sigma_{max}, \sigma_{min}$ Maximum and minimum values of σ.

I. Introduction

The prominent features of solar energy - clean, abundant, and renewable - make photovoltaic (PV) generation popular and promising in various industrial applications [1]. The use of solar energy requires system analysis and optimization to improve the performances of PV installations [2]. These requirements highlight the need to equip PV installations with efficient monitoring equipment and tools, which permit the establishment of data analysis, comparisons, identification, fault events detection [3], [4].

The output power of a PV system is highly dependent on environmental conditions such as solar irradiation and cell temperature. Moreover, it will decrease considerably when mismatch occurs as a result of partial shading, soiling, non-uniform irradiation and cell damage [5]. Among these factors, partial shading is the most significant factor causing mismatch and partial shading scenarios (PSS) are inevitable especially in PV systems installed in urban districts and in areas where low moving clouds are common [6]. The shaded PV cells absorb electric power generated by the insolated cells, leading to hot spots that will irreversible damage the module. Bypassing shaded cells through bypass diodes has been proven to be an effective strategy in protecting against hot spot damage and helping to reduce the decrease of power generation caused by partial shading [7].

The early research on the partial shading condition focuses on understanding PSS and their influence on the mismatch of PV systems [8], [9]. The bypass diodes configurations have been studies in [10], [11]. It is found from these publications that the power-voltage (P-V) characteristics curves exhibit multiple peaks in PSS, and the number of peaks depends on the array topology and bypass diode configurations. Maximum power point (MPP) refers to the operating point on the P-V curve at which the most power is extracted from the PV generator. Studying maximum power point tracking (MPPT) as an optimization problem resulted in using global evolutionary algorithm such as particle swarm optimization [12], simulated annealing [13], [14], differential evolution [15], cuckoo search [16], [17] and firefly algorithm [18] to find the MPP.

Although these global optimization methods have the capability to improve the energy conversion efficiency in PSS, their sampling number is high and there lacks an effective detection and assessment method for monitoring and supervising purposes as well as invoking appropriate model predictive control MPPT algorithms [19]. A sudden big change in output power is normally used as a partial shading occurrence indicator [20]. The simple approach is not capable of distinguish PSS from rapidly changing environmental conditions. In [21], an mathematical expression is used to monitor the equivalent thermal voltage in order to detect partial shading for PV module diagnostics, but it is only applicable for the case of small area shadows. To detect the presence of faults in PV array, Silvestre et al. [22] established reference thresholds based on the errors between simulated and measured capture losses in case of free fault system operation. However, this method does not differentiate between partial shading and short-circuit faults. Ghasemi et al. [23] proposed specified thresholds for detecting PSS in accordance with simulations of many PSS on various structures of PV array. A similar approach is proposed in [24]. The method can detect PSS based on determining the expected values of PV parameters in varying environmental conditions and comparing real-time measurements with these expected values. In [25], abrupt and gradual shading conditions can be identified via equivalent DC impedance of a panel. Li et al. [26] proposed a modified beta method, in which a calculated beta parameter is utilized to detect PSS without setting any additional threshold parameters or periodical interruption.

Since the PV outputs vary with environmental conditions and PV material characteristics, it is not easy to define appropriate thresholds that are applicable for PV systems covering all PSS. In recent years, machine-learning techniques have been introduced to detect partial shadings. These algorithms generally learn the relations between input and output data, and subsequently apply the trained models to perform detection. Machine learning based approaches help overcome the limitation of defining thresholds and aid in the PSS detection [20]. In [27], a decision tree algorithm is used to detect and classify the PV array faults, such as ground fault, line-line fault and mismatch fault caused by PSS. In [28], back-propagation neural network (BPNN) technique is applied to detection and assess PSS in PV arrays. Spataru et al. [29], [30] applied fuzzy inference systems to detect partial shading through the associated increase in series resistance of partially shaded cells. Sarkar and Bakade [31] presented a boundary estimation procedure to recognize the shading pattern, but this method requires additional camera devices and increases the production costs.

Currently available literature focuses on the methods that detect the presence of partial shading in PV systems. However, PSS contains a variety of shading patterns, which lead to different degrees of mismatch loss. Therefore, two important parameters, namely shading rate [28] and shading strength [8], are used to characterize PSS. In this paper, a sorting algorithm is proposed to predict the shading rate and subsequently a multi-output support vector regression is applied to estimate the PSS parameters, including the shading strength as well as the voltage at MPP. Readily available measurements in existing PV systems, such as PV array voltage, current, cell temperature, are used as "attributes" in the training and test set. The proposed method is field tested and validated on a PV system comprising six series-connected PV modules. We demonstrate the practical application of the method to study the PV string in PSS.

In Section II, the electrical characteristics of a PV array, both under uniform irradiation scenarios and PSS, are introduced. Section III presents a shading pattern detection algorithm for PV strings. A multi-output-support vector regression (M-SVR) is used to estimate the shading strength and voltage at the MPP. The accuracy and validity of the proposed method are evaluated in Section IV. Finally, Section V draws the conclusions and perspectives.

II. Electrical Characteristics of a PV String

A. In uniform irradiation scenarios

The basic block for a PV generation psystem is PV module, which comprises a group of PV cells. The PV cell is normally made from silicon doped with minute quantities of boron, phosphorous, gallium, arsenic, or other materials. A PV module is generally modeled by a single-diode equivalent circuit under uniform irradiation scenarios (UIS). On the basis of the Shockley diode representation, the relationship between output current I and voltage V is given by the following nonlinear implicit equation:

$$I = I_{ph} - I_o(e^{\frac{V+Ir_s}{an_sV_t}} - 1) - \frac{V + Ir_s}{r_p}, \tag{1}$$

where I_{ph} is the light-generated current, I_o is the reverse saturation current of diode, a is the ideality factor, r_s is the series resistance, r_p is the parallel resistance and n_s is the number of PV cells in a PV module. With the measured I-V data, the exact values of the five parameters (I_{ph}, I_o, n, r_s and r_p) can be simply extracted by intelligent optimization methods [1], [32], [33]. The V_t is known as thermal voltage, and its value can be estimated as a function of cell temperature T, namely $V_t = BT/e$. The B and e represent the Boltzmann constant (B=1.38065E-23 J/K) and the electron charge (1.60217E-19 C), respectively.

The open circuit voltage is independent of the module area and is limited by the semiconductor properties, thus PV modules are usually connected in series to form a PV string. The electrical characteristics of the string are scaled according to the following rules [34]:

$$\begin{aligned} V_S &= N_S \cdot V, \\ I_S &= I, \\ R_S &= N_S \cdot r_s, \\ R_p &= N_S \cdot r_p, \end{aligned} \tag{2}$$

where V_S, I_S, R_s and R_p denote the voltage, current, series and parallel resistance of the PV string, respectively. The N_S represents the number of modules in the PV string.

The I-V and P-V curves of a 360W PV string varying with different irradiance levels are shown in Fig. 1. It can be seen that the P-V curve obtains only one peak point in UIS. The point on a P-V curve producing the highest output power is known as MPP.

B. In partial shading scenarios

If a PV array is partially shaded by trees, passing clouds, or neighboring buildings, the shaded cells consume power instead of producing power, which leads to "hot-spot" phenomenon. Fig. 2 depicts a PV string comprising 6 modules, which are numbered with M1-M6. The blocking diodes prevent reverse current flow at night. Bypassing shaded cells through bypass diodes has been proven to be an effective strategy in protecting against hot spot damage. For simplicity, it is initially supposed that the array is subjected to two different solar irradiance levels in PSS. The modules that receive a high irradiance level

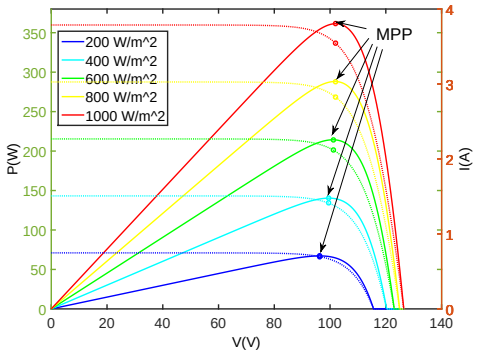

Fig. 1. I-V and P-V curves of a 360W PV string in uniform irradiation scenarios.

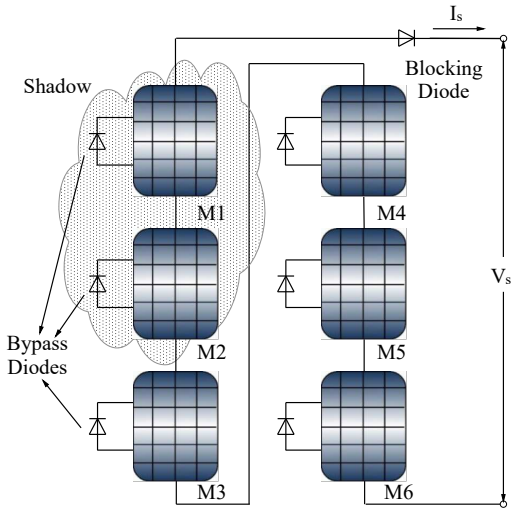

Fig. 2. Schematic diagram of a PV string with bypass diodes.

G_{is} are called insolated modules, and those receiving a low irradiance level G_{sh} are called shaded modules. The partial shading condition can be characterized by two indicators: shading rate χ and shading strength ρ. The shading rate is the percentage of shaded modules in the PV system, expressed by:

$$\chi = \frac{N_{sh}}{N_s}. \tag{3}$$

The shading strength, also named shading factor [28], is defined as the ratio of the irradiation on shaded modules to that on insolated modules [8]:

$$\rho = \frac{G_{\text{sh}}}{G_{\text{is}}}, \tag{4}$$

where N_{sh} is the number of shaded modules in the string. It is assumed that $G_{\text{sh}} = 50\ W/m^2$ and all modules operate at the same temperature as partial shading is not likely to create substantial temperature difference between shaded and insolated modules [28].

Fig. 3(a) demonstrates the I-V and P-V curves of a PV string comprising three shaded module and three insolated

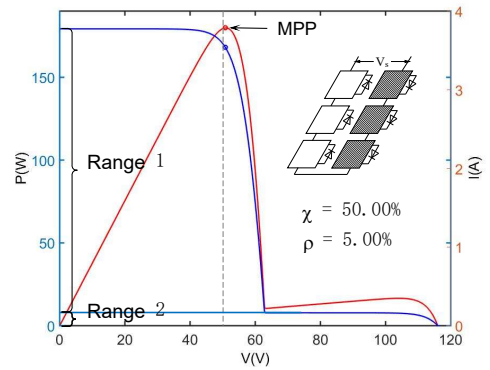

(a) in partial shading scenarios

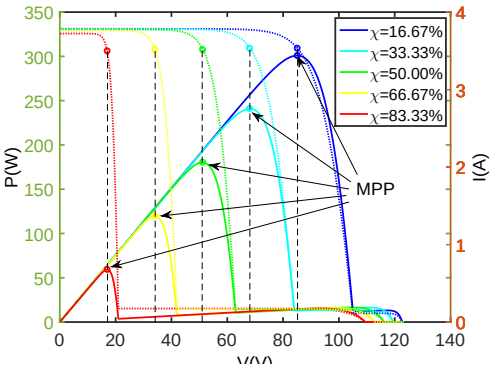

(b) with different χ

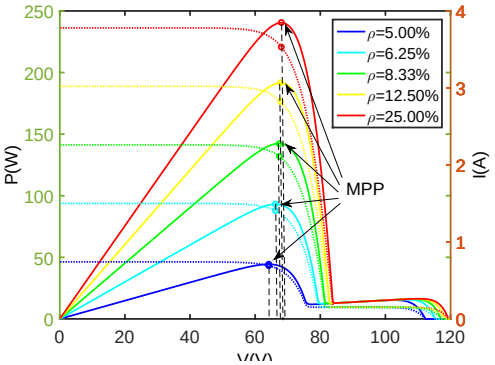

(c) with different ρ

Fig. 3. I-V and P-V curves of a 360W PV string in partial shading scenarios.

modules. When the string current is higher than the short current of shaded modules (Range 1), the current bypasses the shaded modules. The voltage across the diodes is around 0.7 V. On the contrary, when the string current is lower than the short current of shaded modules (Range 2), the insolated modules operate in approximately constant voltage area ranging from the string voltage at MPP $V_{S,mp}$ to string open circuit voltage $V_{S,oc}$.

Fig. 3(b) and 3(c) show the effects of different χ and ρ on I-V and P-V characteristics of a PV string. In Fig. 3(b), the χ varies from 16.67 % to 83.33 %, and ρ is kept constant at 25.00 %. In Fig. 3(b), the ρ varies from 5.00 % to 25.00 %, and the χ is 33.33 %. From the two figures, the locus of V_{mp} can be mathematically expressed as:

$$V_{S,mp} = (N_S - N_{sh})V_{\rm mp} - 0.7N_{sh}\,, \tag{5}$$

where the $V_{S,mp}$ is the string voltage at MPP.

For further discussion, the module voltage-string voltage (V-V_S) characteristics are investigated in Fig. 4, where V_1-V_6 denote the module voltage across M1-M6 respectively, and ΔV_{oc} represents the difference of the open circuit voltage between shaded and insolated modules. Fig. 4 (a) illustrates the V-V_S curves in UIS and Fig. 4 (b)-(d) shows the V-V_S curves in PSS. The module voltages of all modules V_1-V_6 are the same in UIS. In PSS, however, the insolated modules are firstly activated with an increase string voltage. When the module voltage V is approaching its open circuit voltage V_{oc}, the voltage across the shaded modules increases.

Some of the critical observations made from an extensive study of the electrical characteristics of the PV string in Figs. 1 to 4 are listed as follows:

- The value of χ significantly affects the locus of MPP. The greater χ the PV string has, the lower V_{mp} it obtains.
- The ρ has slightly effect on the locus of MPP. A string with smaller ρ leads to a lower V_{mp}.
- Module voltages are identical in UIS.
- The open circuit voltage of insolated modules $V_{\rm oc,is}$ increase with the ρ. The open circuit voltage of shaded modules $V_{\rm oc,sh}$ is assumed to be constant.
- Within the effective range, the voltage difference between shaded and insolated modules is greater than or equal to ΔV_{oc}.

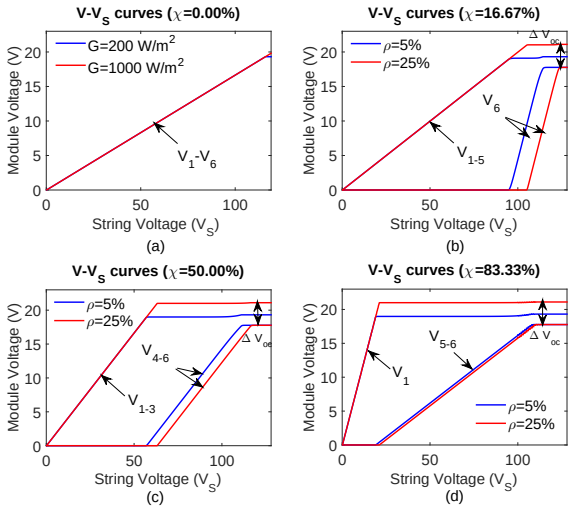

Fig. 4. V-V_S curves of a 360W PV string under different environmental conditions: (a) in UIS: $G = 1000W/m^2$, 25^oC; (b) in PSS: M6 is shaded, $\chi = 16.67\%$, 25^oC; (c) in PSS: M4-M6 are shaded 50.00%, 25^oC; (d) in PSS: M2-M6 are shaded, $\chi = 83.33\%$, 25^oC.

III. Detection and Assessment of Partial Shading Scenarios

The detection and assessment method developed in this work has the capability of identifying the shading factor χ, shading strength ρ, and the voltage at the maximum power point V_{mp}. Fig. 5 shows schematic of the proposed method. A variety of sensors are setup to measure climate variables: cell temperature T and solar irradiance G_{is}. A digital signal procssor (DSP) evaluation board is used to monitor and control a PV string. The integrated maximum power point tracking (MPPT) function is able to record the MPP locus. The shading rate χ is firstly detected via a shading pattern detection algorithm. After formating the training data (including the T, G_{is}, χ, $V_{S,mp}$ and I-V data), the ρ and $V_{S,mp}$ are estimated via an M-SVR.

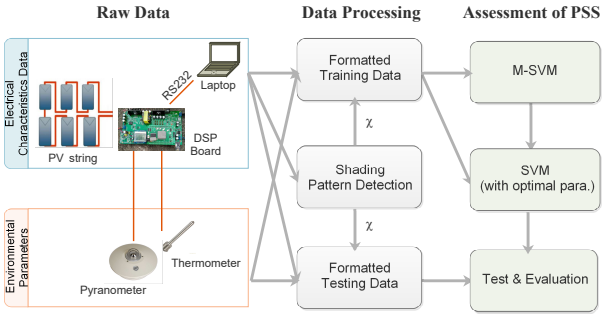

Fig. 5. Schematic of the proposed detection and assessment method of technique scenarios.

A. Shading pattern detection

As explained in the previous section, the shaded modules are not activated until the operating current drops to the magnitude that equals to its short circuit current in PSS. According to this phenomenon, a divide-and-conquer sorting algorithm is proposed to detect the shading pattern of PV strings. Let $\boldsymbol{V} = V[1, ..., N_S]$, a collection of voltage values of PV modules, be the array to be sorted. Suppose $p, r \in [1, N_S]$, and $p \leq r-1$. The basic idea behind the sorting algorithm is to select an element x ($x = V[r]$) as pivot. The $V[x]$ will split the input array $\boldsymbol{V}$ into two sub-arrays: $V[p, ..., q-1]$ and $V[q+1, ..., r]$, so that each element in the left sub-array $V[p, ..., q-1]$ is less than or equal to the middle element $V[q]$ and each element in the right sub-array $V[q+1, ..., r]$ is greater than the middle element $V[q]$. The idea is implemented by a for loop, whose index k is known to run from 1 to $r-1$ and counter j is initialized to $p-1$. When this loop completes, we hold: $A[k] \leq x$, $1 \leq k \leq j$ and $A[k] > x$, $j+1 \leq k \leq r-1$. Then the subroutine outputs the value of q ($q = j+1$). After recursively performing ($\mathrm{sort}(A, p, q-1)$ and $\mathrm{sort}(A, q+1, r)$), the $\mathbf{V}$ is sorted from largest to smallest, and the new array is denoted by $\mathbf{V}_{\mathrm{sort}}$. The first element $\mathrm{sort}[1]$ has the maximum value in the array.

Normalize the $\mathbf{V}_{\mathrm{sort}}$ via (6), so that all the shaded modules are labeled as 1 and others are 0.

$$V_{\mathrm{det}}[i] = \mathrm{round}(V_{\mathrm{sort}}[i]/V_{\mathrm{sort}}[1])\,. \tag{6}$$

The $round$ functions will return either 1 or 0 in accordance with the following rules:

$$V_{\mathrm{det}}[i] = \begin{cases} 1 & V_{\mathrm{sort}}[i]/V_{\mathrm{sort}}[1] \geq \tau \\ 0 & V_{\mathrm{sort}}[i]/V_{\mathrm{sort}}[1] < \tau \end{cases} \tag{7}$$

where τ is a threshold used to differentiate between the UIS and PSS. Based on previous analysis of V-V_S characteristics, the minimum difference between $V_{\mathrm{sort}}[i]$ and $V_{\mathrm{sort}}[1]$ is equal to the difference of the open circuit voltage between shaded and insolated modules ΔV_{oc}. The τ then ban be then defined as:

$$\tau = \min\left(\frac{V_{\mathrm{sort}}[i]}{V_{\mathrm{sort}}[1]}\right) = \frac{V_{\mathrm{oc,sh}}}{V_{\mathrm{oc,is}}}\,. \tag{8}$$

The value of V_{oc} can be roughly calculated by (9).

$$V_{oc} = an_s V_t ln(\frac{I_{ph}}{I_o} + 1). \tag{9}$$

where the r_p is assumed to be positive infinite.

The parameters (such as I_{ph} and I_{o}) can be extracted from I-V data. A number of parameter estimation methods have been proposed in recent literature [32], [35]. As soon as the $\boldsymbol{V}_{\mathrm{det}}$ is determined, the shading rate χ can be calculated as the following equation:

$$\chi = \sum_{i=1}^{N_S} V_{\mathrm{det}_i}/N_S. \tag{10}$$

Algorithm 1 Pseudocode of shading pattern detection algorithm.

Input: $\boldsymbol{V}$
Output: χ and $\boldsymbol{V}_{\mathbf{det}}$
$\boldsymbol{V}_{\mathbf{sort}} = \mathrm{sort}(\boldsymbol{V}, 1, N_S)$
for $i = 1$ TO N_S **do**
  $V_{\mathrm{det}}[i] = \mathrm{round}(V_{\mathrm{sort}}[i]/V_{\mathrm{sort}}[1])$
end for
$\chi = \sum_{i=1}^{N_S} V_{\mathrm{det}_i}/N_S$.
procedure: sort(A, p, r)
if $p < r$ **then**
  x = $A[r]$
  $j = p-1$
  for $k = p$ TO $r-1$ **do**
    if $A[k] \leq x$ **then**
      $j = j+1$
      Exchange $A[j]$ and $A[k]$
    end if
    Exchange $A[j+1]$ and $A[r]$
  end for
  $q = j+1$
  sort(A, p, $q-1$)
  sort(A, $q+1$, r)
end if
return $\boldsymbol{A}$

B. Assessment of partial shading scenarios

A support vector regression (SVR) is used to address the problem of multi-regression estimation for shading rate and factor. The use of a SVR tool will help to exploit the dependencies in measured electrical characteristics and will make each estimates less vulnerable to the measurement errors.

The multi-dimensional input vector $\boldsymbol{x}$ comprises string current I and module voltage vector $\boldsymbol{V}$, and it is normalized within the range 0 to 1 using (11):

$$\boldsymbol{x} = \frac{(\boldsymbol{x} - x_{min})}{x_{max} - x_{min}} \,, \tag{11}$$

where x_{min} and x_{max} represent the maximum and minimum of $\boldsymbol{x}$, respectively.

The χ and ρ are used as output $\boldsymbol{y}$. For a data set consisting of input vectors together with the corresponding output $((\boldsymbol{x}_k, \boldsymbol{y}_k),\ \forall k = 1, ..., n)$, the M-SVR is defined as:

$$\begin{aligned} \min_{w,b,\xi_k,\xi_k^*} \quad & \frac{1}{2} w^T w + C \sum_{k=1}^{n} (\xi_k + \xi_k^*) \\ s.t. \quad & y_k - w^T \phi(x_k) - b \le \varepsilon + \xi_k \\ & w^T \phi(x_k) + b - y_k \le \varepsilon + \xi_k^* \\ & \xi_k, \xi_k^* \ge 0 \end{aligned} \tag{12}$$

where ϕ is a mapping function, C is the associated penalty for excessive deviation, w is the weight vector, b is the bias, ξ_k and ξ_k^* are the non-negative slack variables.

The dual optimization problem can be solved by construction of a Lagrangian function from the primal function with Lagrangian multipliers α, α^*. When the solutions for Lagrangian of (12) (α, α^*, and b) are obtained, the optimization problem leads to the solution:

$$y(x) = \sum_{j=1}^{k} (\alpha_k - \alpha_k^*) K(x, x_k) + b \,, \tag{13}$$

where $K(x, x_k) = \phi(x)^T \phi(x_k)$ is a kernel function, In this paper, we use the radial basis function (RBF) kernel function, expressed by:

$$K(x, x_k) = \exp(-\frac{\|x - x_k\|^2}{\sigma^2}) \,, \tag{14}$$

where σ is a tuning parameter defining the kernel width. Another tuning parameter involved in M-SVR is C. From a multi-objective optimization point of view, M-SVR parameters optimization problem can naturally be described by the root mean square errors (RMSEs):

$$\begin{aligned} \min \quad & \text{RMSE} = \sqrt{\tfrac{1}{n} \textstyle\sum_{k=1}^{n} (y_k - f(x_k))^2} \\ s.t. \quad & C_{min} \le C \le C_{max} \\ & \sigma_{min}^2 \le \sigma^2 \le \sigma_{max}^2 \end{aligned} \tag{15}$$

To analyze the ρ and χ and their influence on partial pattern detection, a good diversity of solutions is necessary. In addition, the context of parameters optimization obtains training and testing the M-SVR for each hyper-parameter set, and a fast non-dominated sorting procedure with less complexity is required to solve (15). In this paper, non-dominated sorting genetic algorithm II (NSGA-II) is used in M-SVR parameter optimization. For more details about the NSGA-II algorithm, we refer to [36].

TABLE I. DATASHEET CHARACTERISTICS OF MSX60 PHOTOVOLTAIC MODULE USED IN SIMULATION AND EXPERIMENTAL VALIDATION.

Parameter	Abbrev.	MSX60	PVM-50	Unit
Maximum Power	P_{max}	60	50	W
Voltage of Pmax	V_{mp}	16.8	18	V
Current at Pmax	I_{mp}	3.56	2.78	A
Open-Circuit Voltage	V_{oc}	21	21.8	V
Short-Circuit Current	I_{sc}	3.87	3.1	A
The no. of cells	n_s	36	36	-
Cell Type		Multi-crystalline	Mono-crystalline	-

IV. RESULTS OF PERFORMANCE EVALUATION

The comprehensive assessment of PSS includes the estimation of the shading strength ρ and shading rate χ, as well as the string voltage at MPP $V_{S,mp}$. In this section, the performance of the proposed method is evaluated in various aspects using simulations and experiments.

A. Simulation Results

A series-connected PV string, which comprises six multicrystal MSX60 PV modules, was constructed in PSIM development environment. The electrical characteristics of MSX60 are given in Table I. All the simulations were performed in MATLAB 2016a on Windows 10 operating system with Intel(R) Core (TM) i7-4770K 3.50GHz CPU and 8G RAM.

Training data contain 6000 operating points covering the ranges of solar irradiation of 200-1000 W/m^2, cell temperature of 25-50 ^oC, shaded modules of 1-5, and shading strength of 6.25%-25%. Table II shows the predicted values of χ as well as the threshold τ used in the pattern detection algorithm. Simulation results indicate the algorithm has accurate detection capabilities for different environment sets.

The M-SVR was invoked to assess the condition by determining the ρ and $V_{S,mp}$ as soon as the shading rate was determined by the shading pattern detection algorithm. NSGA-II was used to obtain optimal parameters C and γ both for ρ and $V_{S,mp}$. Root mean square error (RMSE) was used to quantify the prediction performance. Table III shows ten possible solutions obtained after 300 generations with a population size of 30. Among these optimal solutions, the NSGA-II cannot be optimized to minimize both the RMSE(ρ) and RMSE($V_{S,mp}$). With the aim of obtaining relative low errors of both ρ and $V_{S,mp}$, the parameters C_1, γ_1, C_2, and γ_2 are set to 3.11E+08, 14.70, 2.32E+08, 1.31, respectively.

Fig. 7 demonstrates the distribution of the absolute errors (AEs) E_ρ of ρ and $V_{S,mp}$ at different temperatures in 500 runs. It is observed that the M-SVR show better prediction performance at a temperature approaching the standard test conditions (T = 25 ^oC). The AEs become larger as the temperature arises. On the other side, Fig. 8 further illustrates the distribution of the absolute errors (AEs) E_ρ of ρ and $V_{S,mp}$ at different irradiance levels. The ρ shows higher error at lower

TABLE II. SOLUTIONS WITH NSGA-II ON THE ROTATED PROBLEM

Case	PSS				Detection Results	
	G_H	T	N_{sh}	ρ	τ	χ
1	200	25	1	25.00%	0.93	16.67%
2	200	50	2	25.00%	0.93	33.33%
3	400	25	3	12.50%	0.90	50.00%
4	400	50	4	12.50%	0.89	66.67%
5	600	25	5	8.33%	0.88	83.33%
6	600	50	1	8.33%	0.87	16.67%
7	800	25	2	6.25%	0.86	33.33%
8	800	50	3	6.25%	0.85	50.00%
9	1000	25	4	5.00%	0.85	66.67%
10	1000	50	5	5.00%	0.84	83.33%

irradiance level, but irradiance level hasn't had much impact the average prediction ability in prediction of the $V_{S,mp}$.

It is worth pointing out that the proposed method not only delivers useful environmental information in PSS, but also has the capability to predict the voltage corresponding to maximum power point $V_{S,mp}$. Fig. 9 illustrates the AEs of $V_{S,mp}$ from the best results in 500 runs. As shown in Figs. 9 (a)-(f), the number of shaded modules of the PV string was varied from 0 to 5 yielding 6 different shading patterns ($\chi = 0\%$, $\chi = 16.67\%$, $\chi = 33.33\%$, $\chi = 50\%$, $\chi = 66.67\%$, $\chi = 83.33\%$). The AEs were evaluated under various irradiations ($200W/m^2$, $600W/m^2$, $800W/m^2$, $1000W/m^2$) and temperatures (0^oC, 25^oC, 50^oC, 75^oC).

Some of the critical observations made from an extensive study of the best results in Fig. 9 are listed as follows (i) the AEs are relatively large when the V_S is within the range $V_{S,mp}$-$V_{S,oc}$ in UIS; (ii) the AEs of $V_{S,mp}$ are relatively large as the shaded modules are activated in PSS; (iii) the string voltage obtaining maximum AE for $V_{S,mp}$ gets smaller with the increase of χ in PSS; (iv) the string voltage obtaining maximum AE for $V_{S,mp}$ becomes smaller with the increase of cell temperature. It is because the value of V_{oc} decreases when the temperature rises; (v) the proposed method has similar prediction performance in UIS and PSS. The mean absolute error (MAE) of $V_{S,mp}$ in PSS is 0.4 % lower than that of $V_{S,mp}$ in UIS.

Training data sets is often a time-consuming process, and therefore it is commonly assumed that the training time is an important objective metric for evaluating the computational efficiency. Fig. 6 compares the training time of M-SVR and BPNN [28] over ten runs with respect to the amount of training data. Using the same settings as [28], a three-layer BPNN were constructed together with a tansigmoidal activation function. There are 20 neurons used in the hidden layer. In this experiment, the M-SVR spends only about one tenth of BPNN training time. It is worth pointing out that the time complexity of BPNN is more tunable with choice of the BPNN structure. In general, both BPNN and M-SVR on a single processor have a time complexity of $O(n^3)$. The complexity of BPNN mainly depends on the count of weights in the network, while the complexity of M-SVR mainly depends on the number of support vectors.

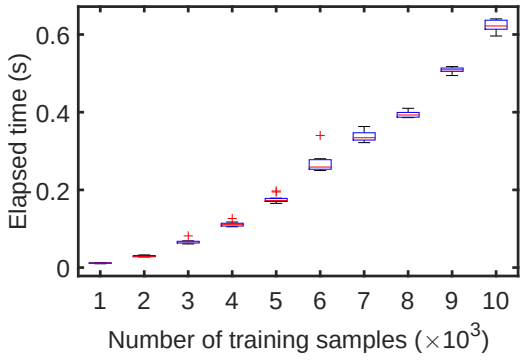

(a) M-SVR

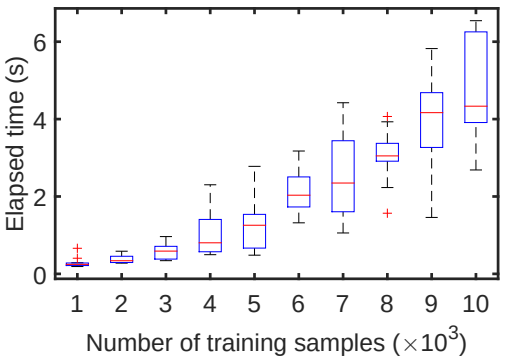

(b) BPNN

Fig. 6. Training time of M-SVR and BPNN.

TABLE III. SIMULATION RESULTS OF SHADING PATTERN DETECTION ALGORITHM.

C_1	C_2	γ_1	γ_2	ρ	$V_{S,mp}$
3.11E+08	2.32E+08	14.70	1.31	1.16E-02	9.20E-01
2.51E+08	2.2E+08	14.70	1.23	1.18E-02	1.00E+00
2.34E+08	2.22E+08	14.89	1.34	1.24E-02	1.01E+00
2.98E+08	2.39E+08	13.69	9.89	1.25E-02	3.39E+00
2.99E+08	2.57E+08	13.47	27.23	1.31E-02	4.42E+00
2.41E+08	2.23E+08	14.69	1.82	1.31E-02	1.08E+00
2.51E+08	2.2E+08	14.70	1.23	1.33E-02	9.09E-01
3.24E+08	2.33E+08	14.70	1.83	1.38E-02	1.24E+00
2.44E+08	2.22E+08	16.89	1.31	1.60E-02	9.72E-01
2.25E+08	1.97E+08	54.21	1.15	2.66E-02	9.36E-01

B. Experimental Results

The simulation results show that the proposed method is capable of detecting and assessing of partial shading scenarios with acceptable accuracy. However, the I-V characteristics of a PV string vary with different temperature and irradiance, as well as shading rate. The simulations only consider several specific environmental conditions. To evaluate the prediction performance of the proposed method on real-time PV controller, more experimental tests were conducted on a PV string comprising four series-connected mono-crystalline PV modules with the datasheet characteristics shown in Table I.

Fig. 10 (a) and (b) show the experimental setup. Table IV shows the main components used in experimental setup. The

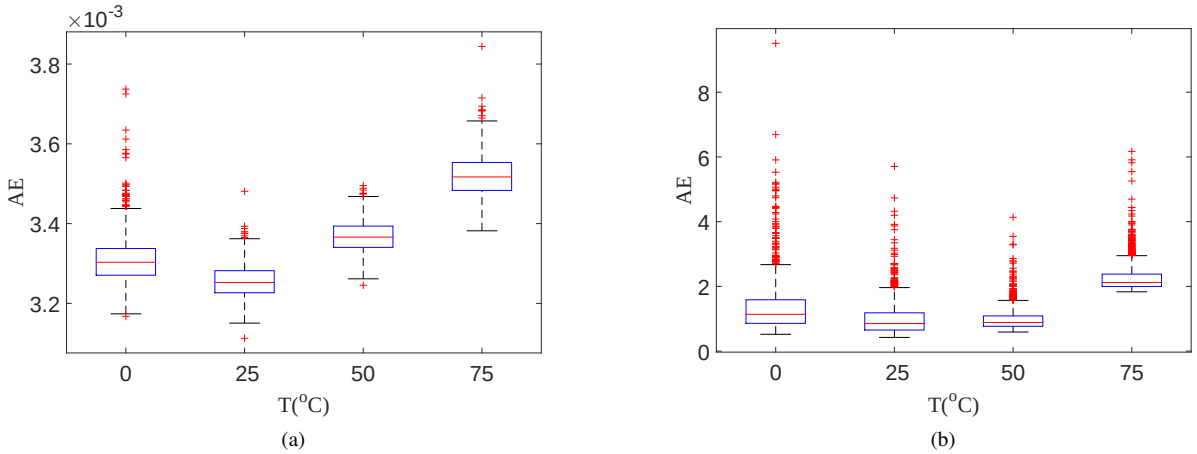

Fig. 7. Statistics of the AEs at different temperatures of the evaluated methods (a) ρ (b) $V_{S,mp}$.

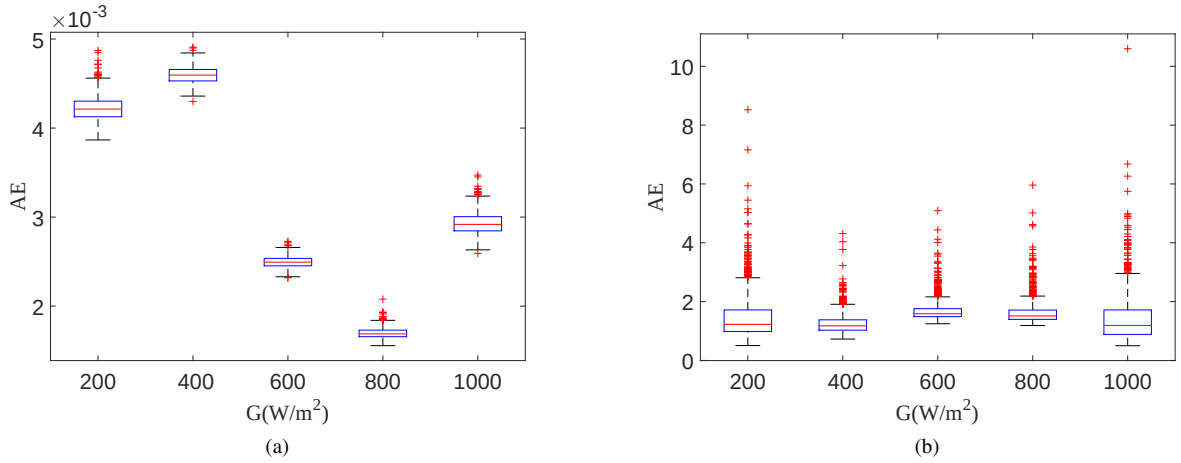

Fig. 8. Statistics of the AEs at different irradiance levels of the evaluated methods (a) ρ (b) $V_{S,mp}$.

terminal current and voltage of the PV string were measured using an intelligent electronic load REK RK8511, offering a wide range of resistance 0.03-10 ohm. In this experiment, the resistance was set to 60 Ω. The DS18B20 digital thermometer, providing 9-bit to 12-bit Celsius temperature measurements, was used as temperature sensor. The WXL-FZD pyranometer is a cost-effective tool for measurement of solar radiation in Watt per square meter (W/m^2). The micro-controller used for data processing is TMS320F28335, a 32-bit floating-point DSP featuring 16 channels for analog-to-digital converter (ADC) module with 12-bit resolution and a varied group of series port peripherals, including 1 serial peripheral interface (SPI) module, 1 inter-integrated circuit (I2C) bus, and 3 serial communication interface (SCI/UART) modules, etc. This experimental system incorporates a global maximum power point tracking algorithm [37] to find the MPP in PSS and UIS.

The optimal parameters C and γ were firstly obtained via the NSGA-II. After 300 generations with a population size of 30, 18 non-dominated solutions were obtained. Pareto-optimal region is shown in Fig. 11. A compromise was made between the errors of both parameters in this paper. The C_1, γ_1, C_2 and γ_2 were set to 8.6789E4, 6.2037E3, 3.2442E4, and 3.1306E3 respectively.

Fig. 12 shows the resulting shading rate, shading strength, and voltage at the MPP in Suzhou University of Science and Technology at latitude 31.249281^o N and longitude 120.576731^o E. The environmental conditions T and ρ were recorded every 15 minutes in a typical daylight (7:00-17:00). During the test, the shading rate was set to different values ($\chi = 0$ %, $\chi = 25$ %, $\chi = 50$ %$\chi = 75$ %). The results given by the presented method were compared with the detection results related to the same experimental system using BPNN. The results obtained by the BPNN and M-SVR are marked with asterisks and circles, respectively. The dotted lines represent measured data. From Fig. 12, it is observed that both the proposed shading pattern detection algorithm and the BPNN can successfully detect the PSS and UIS. In the estimation of the ρ, the M-SVR obtains lower RMSE than

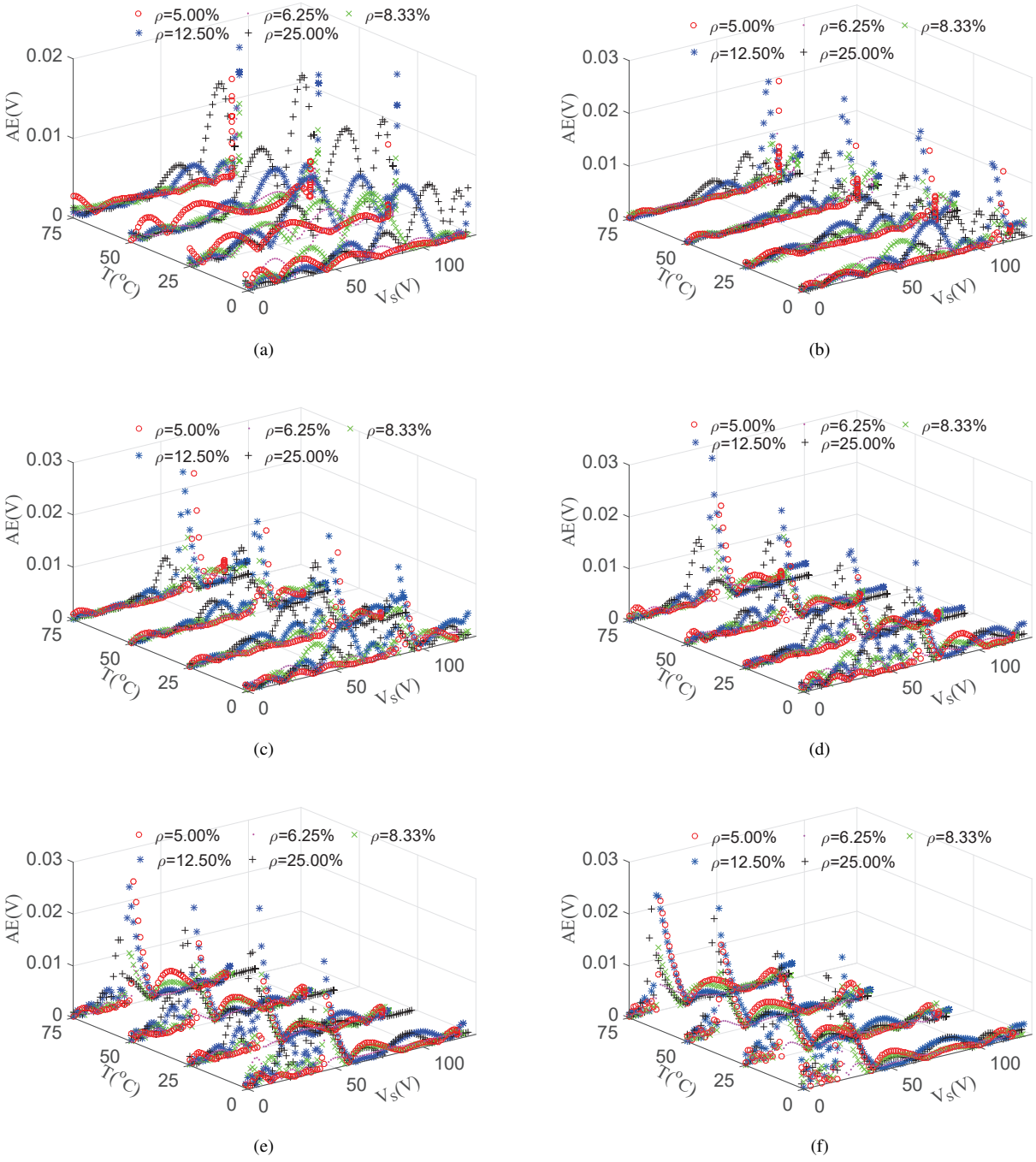

Fig. 9. AEs of $V_{S,mp}$ under various environmental conditions (a) $\chi = 0\%$ (b) $\chi = 16.67\%$ (c) $\chi = 33.33\%$ (d) $\chi = 50\%$ (e) $\chi = 66.67\%$ (f) $\chi = 83.33\%$

the BPNN. A relative big shading strength error occurs when the χ reaches its minimum or maximum. There is a good match between the measured data and the estimated results $V_{S,mp}$ by the M-SVR. The RMSE of the BPNN is 23.42% higher than that of M-SVR. The figure indicates remarkable effectiveness in assessing shaded modules in PSS. It's worth highlighting that all the testing data in PSS do not belong to training data, and thus the errors are slight higher than that obtained in simulations.

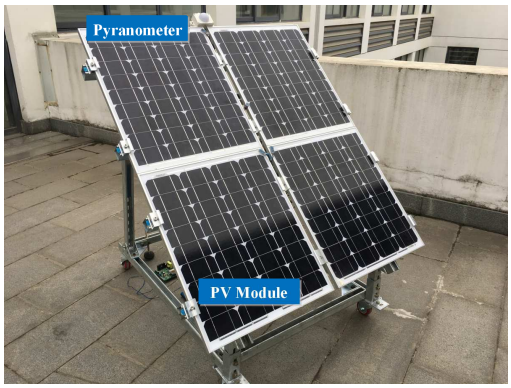

(a)

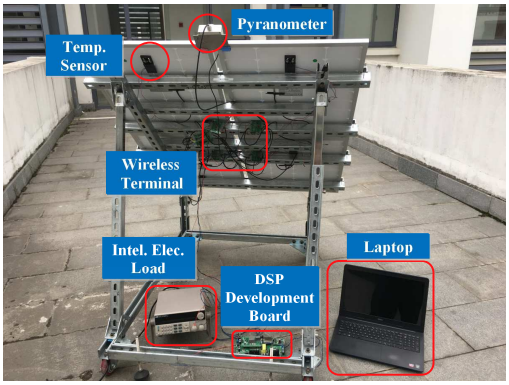

(b)

Fig. 10. Overview of experimental setup.

TABLE IV. EXPERIMENTAL SETUP COMPONENTS.

Component	Off-the-shelf part #
PV module	PVM-50
Temerature Sensor	DS18B20
Pyranometer	WXL-FZD
Voltage Transducer	LV25-P
Current Transducer	LA25-NP
DSP	TMS320F28335
Intelligent Electronic Load	ReK RK8511
Other components	Connects, cases, etc.

V. CONCLUSION

The paper has presented a method for the detection and assessment of PSS in PV strings. The PSS is characterized by the shading rate and shading strength. A partial shading detection

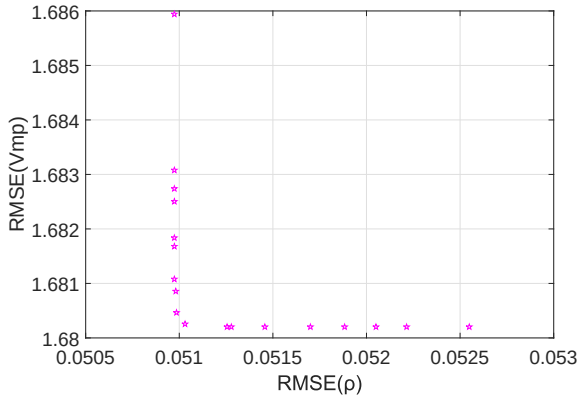

Fig. 11. Pareto-optimal front using NSGA-II.

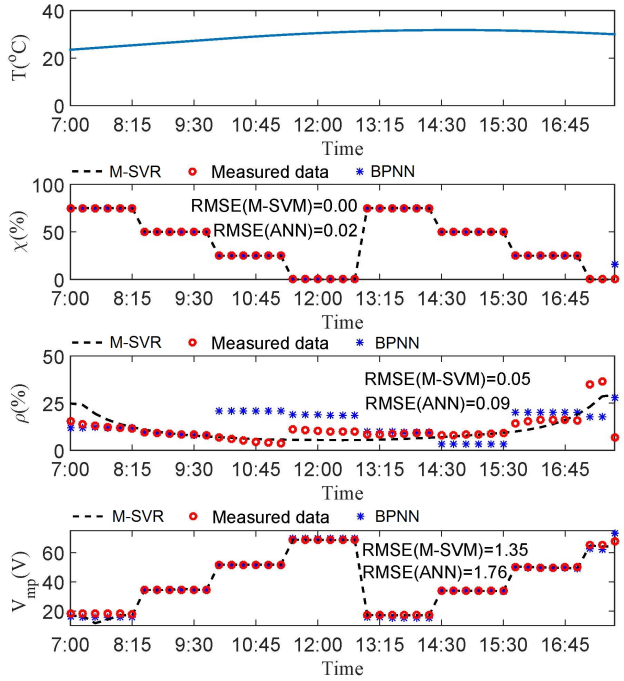

Fig. 12. Experimental results for the 10 hours (7:00 - 18:00) (a) T (b) χ (c) ρ and (d) $V_{S,mp}$

algorithm has been proposed to identify the shading rate. In case the number of shaded modules is determined, an M-SVR is applied to fully assess the shading strength and voltage at the MPP. Simulations show that the proposed method has an excellent prediction performance. An experimental system was set up to investigate the predict performance of the proposed method with a variety of shading patterns. Experimental results show that the proposed method could be straightforwardly extended to cover various operating ranges of the given PV array, or to consider other string topologies as well. The RMSE of the proposed method is at least 20 % lower than that

of BPNN in the detection of ρ and $V_{S,mp}$. In future work, experimental tests of the proposed method could highlight the solutions for partial shading scenarios using different serial and parallel connections.

ACKNOWLEDGMENT

The authors would like to thank the anonymous reviewers for their invaluable comments to improve this manuscript. This research is supported by the National Natural Science Foundation of China (Grant No. 61702353), the Natural Science Foundation of Jiangsu Province (Grant No. BK20160355), the Science and Technology Project of Ministry of Housing and Urban-Rural Development (Grant No. 2016-K1-019), and , and the Key Program Special Fund in XJTLU (Grant No. KSF-A-01).

REFERENCES

[1] J. Ma, K. L. Man, S. U. Guan, T. O. Ting, and P. W. H. Wong, "Parameter estimation of photovoltaic model via parallel particle swarm optimization algorithm," *International Journal of Energy Research*, vol. 40, no. 3, 2015.

[2] H. Mekki, A. Mellit, and H. Salhi, "Artificial neural network-based modelling and fault detection of partial shaded photovoltaic modules," *Simulation Modelling Practice and Theory*, vol. 67, pp. 1–13, 2016.

[3] B. P. Kumar, G. S. Ilango, M. J. B. Reddy, and N. Chilakapati, "Online fault detection and diagnosis in photovoltaic systems using wavelet packets," *IEEE Journal of Photovoltaics*, vol. 8, no. 1, pp. 257–265, Jan 2018.

[4] M. Dez-Mediavilla, C. Alonso-Tristn, M. C. Rodrguez-Amigo, T. Garca-Caldern, and M. I. Dieste-Velasco, "Performance analysis of pv plants: Optimization for improving profitability," *Energy Conversion and Management*, vol. 54, no. 1, pp. 17–23, 2012.

[5] K. Hu, W. Li, L. Wang, F. Zhu, and Z. Shou, "Topology and control strategy of power optimisation for photovoltaic arrays and inverters during partial shading," *IET Generation, Transmission Distribution*, vol. 12, no. 1, pp. 62–71, 2018.

[6] A. Dolara, G. C. Lazaroiu, S. Leva, and G. Manzolini, "Experimental investigation of partial shading scenarios on pv (photovoltaic) modules," *Energy*, vol. 55, no. 55, pp. 466–475, 2013.

[7] R. Ahmad, A. F. Murtaza, H. A. Sher, U. T. Shami, and S. Olalekan, "An analytical approach to study partial shading effects on pv array supported by literature," *Renewable and Sustainable Energy Reviews*, vol. 74, pp. 721 – 732, 2017.

[8] M. A, x00E, ki, and S. Valkealahti, "Power losses in long string and parallel-connected short strings of series-connected silicon-based photovoltaic modules due to partial shading conditions," *IEEE Transactions on Energy Conversion*, vol. 27, no. 1, pp. 173–183, 2012.

[9] J. Ahmed and Z. Salam, "An accurate method for mppt to detect the partial shading occurrence in a pv system," *IEEE Transactions on Industrial Informatics*, vol. 13, no. 5, pp. 2151–2161, 2017.

[10] H. Zheng, S. Li, R. Challoo, and J. Proano, "Shading and bypass diode impacts to energy extraction of pv arrays under different converter configurations," *Renewable Energy*, vol. 68, no. 7, pp. 58–66, 2014.

[11] S. Silvestre, A. Boronat, and A. Chouder, "Study of bypass diodes configuration on pv modules," *Applied Energy*, vol. 86, no. 9, pp. 1632–1640, 2009.

[12] L. Yi-Hwa, H. Shyh-Ching, H. Jia-Wei, and L. Wen-Cheng, "A particle swarm optimization-based maximum power point tracking algorithm for pv systems operating under partially shaded conditions," *IEEE Transactions on Energy Conversion*, vol. 27, no. 4, pp. 1027–1035, 2012.

[13] M. Miyatake, M. Veerachary, F. Toriumi, N. Fujii, and H. Ko, "Maximum power point tracking of multiple photovoltaic arrays: A pso approach," *IEEE Transactions on Aerospace and Electronic Systems*, vol. 47, no. 1, pp. 367–380, 2011.

[14] S. Lyden and M. E. Haque, "A simulated annealing global maximum power point tracking approach for pv modules under partial shading conditions," *IEEE Transactions on Power Electronics*, vol. 31, no. 6, pp. 4171–4181, 2016.

[15] M. F. N. Tajuddin, S. M. Ayob, Z. Salam, and M. S. Saad, "Evolutionary based maximum power point tracking technique using differential evolution algorithm," *Energy and Buildings*, vol. 67, no. 0, pp. 245–252, 2013. [Online]. Available: http://www.sciencedirect.com/science/article/pii/S0378778813004763

[16] J. Ahmed and Z. Salam, "A maximum power point tracking (mppt) for pv system using cuckoo search with partial shading capability," *Applied Energy*, vol. 119, no. 12, pp. 118–130, 2014.

[17] B. R. Peng, K. C. Ho, and Y. H. Liu, "A novel and fast mppt method suitable for both fast changing and partially shaded conditions," *IEEE Transactions on Industrial Electronics*, vol. 65, no. 4, pp. 3240–3251, April 2018.

[18] K. Sundareswaran, S. Peddapati, and S. Palani, "Mppt of pv systems under partial shaded conditions through a colony of flashing fireflies," *IEEE Transactions on Energy Conversion*, vol. 29, no. 2, pp. 463–472, 2014.

[19] M. A. Ghasemi, H. M. Foroushani, and M. Parniani, "Partial shading detection and smooth maximum power point tracking of pv arrays under psc," *IEEE Transactions on Power Electronics*, vol. 31, no. 9, pp. 1–1, 2015.

[20] J. Ma, T. Zhang, Y. Shi, X. Li, and H. Wen, "Shading pattern detection using electrical characteristics of photovoltaic strings," in *2016 IEEE International Conference on Power Electronics, Drives and Energy Systems (PEDES)*, 2016, pp. 1–4.

[21] D. Sera, R. Teodorescu, and P. Rodriguez, "Partial shadowing detection based on equivalent thermal voltage monitoring for pv module diagnostics," in *35th Annual Conference of IEEE Industrial Electronics (IECON09)*, 2009, Conference Proceedings, pp. 708–713.

[22] S. Silvestre, A. Chouder, and E. Karatepe, "Automatic fault detection in grid connected pv systems," *Solar Energy*, vol. 94, no. 4, pp. 119–127, 2013.

[23] M. A. Ghasemi, H. M. Forushani, and M. Parniani, "Partial shading detection and smooth maximum power point tracking of pv arrays under psc," *IEEE Transactions on Power Electronics*, vol. 31, no. 9, pp. 6281–6292, 2016.

[24] N. Gokmen, E. Karatepe, S. Silvestre, B. Celik, and P. Ortega, "An efficient fault diagnosis method for pv systems based on operating voltage-window," *Energy Conversion and Management*, vol. 73, no. 5, pp. 350–360, 2013.

[25] T. Ghanbari, "Permanent partial shading detection for protection of photovoltaic panels against hot spotting," *IET Renewable Power Generation*, vol. 11, no. 1, pp. 123–131, 2017.

[26] X. Li, H. Wen, Y. Hu, L. Jiang, and W. Xiao, "Modified beta algorithm for gmppt and partial shading detection in photovoltaic systems," *IEEE Transactions on Power Electronics*, vol. 33, no. 3, pp. 2172–2186, March 2018.

[27] Y. Zhao, L. Yang, B. Lehman, and J. F. De Palma, "Decision tree-based fault detection and classification in solar photovoltaic arrays," in *Applied Power Electronics Conference and Exposition*, 2012, Conference Proceedings, pp. 93–99.

[28] F. Salem and M. A. Awadallah, "Detection and assessment of partial shading in photovoltaic arrays," *Journal of Electrical Systems & Information Technology*, vol. 3, no. 1, pp. 23–32, 2016.

[29] S. Spataru, D. Sera, T. Kerekes, and R. Teodorescu, "Detection of increased series losses in pv arrays using fuzzy inference systems," in *38th IEEE Photovoltaic Specialists Conference (PVSC)*, 2012, Conference Proceedings, pp. 464–469.

[30] ——, "Diagnostic method for photovoltaic systems based on light iv measurements," *Solar Energy*, vol. 119, pp. 29–44, 2015.

[31] G. Sarkar, "Analysis of shading pattern of solar panels," *Ijret Org*, vol. 03, no. 2, pp. 594–599, 2014.

[32] J. Ma, Z. Bi, T. O. Ting, S. Hao, and W. Hao, "Comparative performance on photovoltaic model parameter identification via bio-inspired algorithms," *Solar Energy*, vol. 132, pp. 606–616, 2016.

[33] J. Ma, T. O. Ting, K. L. Man, N. Zhang, S. U. Guan, and P. W. H. Wong, "Parameter estimation of photovoltaic models via cuckoo search," *Journal of Applied Mathematics*, vol. 2013, no. 2, pp. 1–11, 2013.

[34] L. Castaner and S. Silvestre, *Modelling Photovoltaic Systems Using PSpice*. John Wiley & Sons Ltd., 2002.

[35] M. G. Villalva, J. R. Gazoli, and E. R. Filho, "Comprehensive approach to modeling and simulation of photovoltaic arrays," *IEEE Transactions on Power Electronics*, vol. 24, no. 5, pp. 1198–1208, 2009.

[36] K. Deb, A. Pratap, S. Agarwal, and T. Meyarivan, "A fast and elitist multiobjective genetic algorithm: Nsga-ii," *IEEE Transactions on Evolutionary Computation*, vol. 6, no. 2, pp. 182–197, 2002.

[37] C. Liang-Rui, T. Chih-Hui, L. Yuan-Li, and L. Yen-Shin, "A biological swarm chasing algorithm for tracking the pv maximum power point," *IEEE Transactions on Energy Conversion*, vol. 25, no. 2, pp. 484–493, 2010.